ENGN8602 FINAL REPORT

Pengfei Fang(u5765437)

Research School of Engineering

The Australian National University

SUPERVISORY PANEL:

Dr. Zhiyong Sun,

Assoc. Prof. Changbin (Brad) Yu

EXAMINER:

Dr. Qingchen Liu

Contents

1 Introduction

In recent years, research on the multi-agent consensus problems [1] under practical constraints is gaining much attention due to its closed connection to industrial applications. By practical constraints, mainly three types are considered, namely agent dynamics constraints, actuator constraints and communication/sensing constraints [2]. Among them, actuator constraints and communication/sensing constraints arise from the scenarios where agents are equipped with digital devices (processors, actuators, sensors and wireless transmitters/receivers) with limited performance. To deal with these practical constraints, time-scheduled [3, 4] and event-scheduled [5, 6, 7] control schemes have been introduced. Compared to time-scheduled control, event-scheduled control is more favourable in multi-agent systems since it provides aperiodic event triggers for information broadcasting and controller updates, which can reduce the requirement of on-board resources significantly.

From the viewpoint of the controller update, there are *three* main event-triggered schemes, which are widely adopted among vast numbers of papers regarding event-triggered multi-agent consensus problem [5, 6, 8, 9, 7, 10]. The first scheme is proposed in [5] where each agent triggers events and broadcasts its event times to its neighbours; the controller for each agent *is updated both at its own event times as well as the event times of its neighbours*. We refer interested readers to the follow-up work [8, 9], where time-dependent trigger conditions and a time regulation idea are respectively introduced to obtain Zeno-free triggers (Zeno behaviour is excluded for each agent). The second scheme proposed in [6] and developed in [11, 12] requires each agent to continuously measure the relative information over its edge links; by using combined relative measurements to design trigger condition, each agent only needs to *update its control input at its own event times*. The third scheme proposed in [7, 10] is also termed the edge-event-based triggering scheme. Trigger events are defined over each edge link and activate *the controller updates for two linked agents simultaneously*. Zeno-free triggers are achieved by using a switching edge weight approach. The work of [13] extends the results in [7, 10] by considering directed graph and double integrator agent dynamics. Time-dependent trigger condition is used to eliminate Zeno behaviour rather than the instead of weight approach.

Note that two issues are not well addressed in all of the above mentioned work: 1) the discussion of global or local coordinate frames for information sensing, and 2) the assumption that all agents use synchronized clocks. In [14], the authors provide explana-

tions about the coordinate frame requirements for [5, 8, 9, 6, 11]. However, this issue is not addressed in papers [7, 10] using edge-event-based schemes. On the other hand, the assumption of synchronized clocks is actually not reflective of many practical applications (e.g. robots are not likely be activated simultaneously). Achieving clock synchronization is a challenging task [15, 16]. We emphasize that the assumption of synchronized clocks plays a very important role in edge-event-based trigger scheme [7, 10, 13]. This is because two agents linked by one edge cannot trigger events simultaneously if they do not work under synchronized clocks i.e. synchronous controller updates for two linked agents cannot be guaranteed.

In this report, we present novel edge-event-based algorithms to achieve multi-agent consensus with Zeno-free triggers under both synchronized and unsynchronized clocks. The agent's dynamics are modelled by single integrators and the graph topology is assumed to be fixed, undirected and connected. The contributions of this report is two-fold. Firstly, as compared to [7, 10], the synchronized clock case studied in section 3 and section 4 provides another point of view with much simpler trigger conditions both for undirected and directed sensing topologies. In our framework, agents only use relative information measured in its own local coordinate frame to achieve *average consensus* in undirected sensing topologies and *consensus* in directed sensing topologies. This is in contrast to prior work [17, 9] (a global coordinate frame is required for all agents) and [6, 11] (average consensus cannot be achieved). We also apply the time regulation idea from [11] to guarantee Zeno-free triggers, which differs from the time-dependent trigger condition used in [13]. Secondly, the unsynchronized clock case studied in Section 5 provides a generalised framework for edge-event-based triggering scheme. The case involving synchronized clocks thus can be regarded as a special case. In this generalised framework, each agent measures the relative information and updates the control input under its own isolated clock. Edge events are defined over an individual agent rather than two linked agents, i.e. two agents linked by one edge do not update their control inputs synchronously. To the authors' knowledge, similar results are not found in the literature.

The rest of this report is structured as follows. Chapter 2 provides mathematical notation and background on graph theory. In Chapter 3 to 5, the synchronized clock case and the unsynchronized clock case are explained with details, respectively. Numerical simulations are provided at the end of the each chapter to verify the effectiveness of the proposed strategies. Finally, Chapter 6 concludes this paper and indicates a future research topic.

2 Preliminaries and background

2.1 Notations

In this part, some basic notations are introduced. Let $\mathbb{N}$, $\mathbb{R}$ and $\mathbb{R}^n$ denote the natural number set, real number set and the n-dimensional real Euclidean space, respectively. The set of $m \times n$ real matrices is denoted by $\mathbb{R}^{m\times n}$. The empty set is denoted by $\emptyset$. The transpose of a vector or matrix M is denoted by M^T. $\lambda_i(M)$ denotes the i-th smallest eigenvalue of a symmetric matrix M. I_n is the $n \times n$ identity matrix. The Euclidean norm of a vector, and the matrix norm induced by the Euclidean norm, is denoted by $\|\cdot\|$.

2.2 Graph theory

2.2.1 Undirected graph

A group of n agents is modelled by an undirected graph $\mathcal{G}$ with vertex set $\mathcal{V} = \{v_1, v_2, \ldots, v_n\}$ and edge set $\mathcal{E} = \{\epsilon_1, \epsilon_2, \ldots, \epsilon_m\} \subset \mathcal{V}\times\mathcal{V}$. A path in graph $\mathcal{G}$ from vertex v_{i_1} to vertex v_{i_j} is a sequence of distinct vertices starting from v_{i_1} and ending with v_{i_j} such that $(v_{i_k}, v_{i_{k+1}}) \in \mathcal{E}$ for $k = 1, 2, \ldots, j-1$. A graph is called connected if there is a path between any two vertices. N_i, the neighbour set of node v_i, is defined as $N_i = \{v_j \in \mathcal{V} : (v_i, v_j) \in \mathcal{E}\}$. The adjacency matrix $A \in \mathbb{R}^{n\times n}$ of graph $\mathcal{G}$ indicates the vertex adjacency relationship, with entries $a_{ij} = 1$ if $(v_i, v_j) \in \mathcal{E}$, and $a_{ij} = 0$ otherwise. Let D be the $n \times n$ diagonal matrix of d_i's, where the degree d_i of each vertex i is given by $d_i = \sum_{j=1}^{n} a_{ij}$. The Laplacian matrix of G is a symmetric positive semi-definite matrix given by $L = D - A$. For a connected graph, the eigenvalues of L are denoted by $0 = \lambda_1(L) < \lambda_2(L) \leq \ldots \leq \lambda_n(L)$.

Label the m edges from 1 to m and each edge is assigned an arbitrary orientation. Each entry of the $m \times n$ incidence matrix H of graph $\mathcal{G}$ are defined as

$$h_{ra} = \begin{cases} 1, & \text{if node } v_a \text{ is the terminal node of } r\text{-th edge} \\ -1, & \text{if node } v_a \text{ is the initial node of } r\text{-th edge} \\ 0, & \text{otherwise} \end{cases} \tag{1}$$

The incidence matrix H can be divided into two sub matrices: the in-incidence matrix and the out-incidence matrix. Following the definitions in [18], each entry of the $m \times n$

in-incidence matrix $H_{\odot}$ [18] is denoted as

$$(h_{\odot})_{ra} = \begin{cases} 1, & \text{if node } v_a \text{ is the terminal node of } r\text{-th edge} \\ 0, & \text{otherwise} \end{cases} \tag{2}$$

and each entry of the $m \times n$ out-incidence matrix $H_{\otimes}$ is denoted as

$$(h_{\otimes})_{ra} = \begin{cases} -1, & \text{if node } v_a \text{ is the initial node of } r\text{-th edge} \\ 0, & \text{otherwise} \end{cases} \tag{3}$$

It is obvious that $H = H_{\odot} + H_{\otimes}$.

Let $x_i \in \mathbb{R}$ denote a state that is assigned to agent i. The stack state vector $x = [x_1, x_2, \cdots, x_n]^T \in \mathbb{R}^n$ records all agents' states. It is well known that the relative state vector can be constructed as:

$$z = Hx \tag{4}$$

where $z = [z_1, z_2, \cdots, z_m]^T \in \mathbb{R}^m$, with $z_r \in \mathbb{R}$ being the relative state over ϵ_r.

Example 1. *We show an example of an undirected graph to illustrate the derivation of the equation described above. Consider an undirected graph with 4 nodes and 4 edges shown in figure 1. For the purpose of writing an oriented incidence matrix, we assign an orientation to each edge arbitrarily, which is shown in figure 2.*

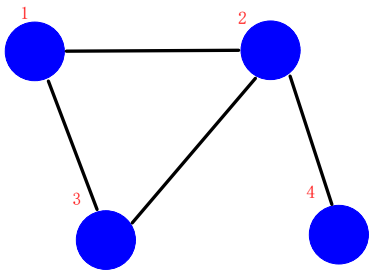

Figure 1: Undirected graph.

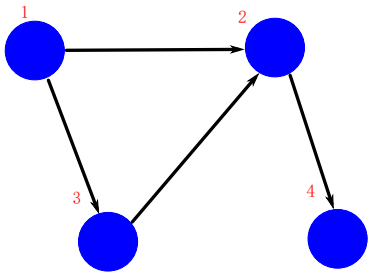

Figure 2: Directed graph with assigned an orientation to each edge.

The orientated incidence matrix H for the undirected graph in figure 1 can be obtained in (5)*. Furthermore, the associated in-incidence matrix $H_{\odot}$ and out-incidence matrix $H_{\otimes}$ can also been obtained in* (6) *and* (7)*, respectively. It is obvious that the equation $H = H_{\odot} + H_{\otimes}$ holds.*

$$H = \begin{bmatrix} -1 & 1 & 0 & 0 \\ -1 & 0 & 1 & 0 \\ 0 & 0 & -1 & 1 \\ 0 & -1 & 0 & 1 \end{bmatrix} \tag{5}$$

$$H_{\odot} = \begin{bmatrix} 0 & 1 & 0 & 0 \\ 0 & 0 & 1 & 0 \\ 0 & 0 & 0 & 1 \\ 0 & 0 & 0 & 1 \end{bmatrix} \tag{6}$$

$$H_{\otimes} = \begin{bmatrix} -1 & 0 & 0 & 0 \\ -1 & 0 & 0 & 0 \\ 0 & 0 & -1 & 0 \\ 0 & -1 & 0 & 0 \end{bmatrix} \tag{7}$$

The relative state vector is the defined according to (4)*. As an example, one has $z_1 = x_2 - x_1$, i.e. the vector at edge ϵ_1 is defined by the relative state between agent* 2 *and agent* 1*.*

For an undirected graph, we have the following lemma:

Lemma 2.1. *[19] If graph $\mathcal{G}$ is undirected and connected, the Laplacian matrix L can be given by $L = H^T H$. The matrix HH^T and the Laplacian matrix L both have non-negative eigenvalues and moreover the same positive ones.*

Lemma 2.2. *[19] If graph $\mathcal{G}$ is undirected and connected, then $z^T HH^T z \geq \lambda_2(L)\|z\|^2$, where $\lambda_2(L)$ refers to the smallest positive eigenvalue of Laplacian matrix L.*

2.2.2 Directed graph

In order to analyze directed sensing topologies, it is necessary to refine some definitions for the undirected graph. A group of n agents is modeled by an directed graph $\mathcal{D}$ with vertex set $\mathcal{V} = \{v_1, v_2, \ldots, v_n\}$ and edge set $\mathcal{E} = \{\epsilon_1, \epsilon_2, \ldots, \epsilon_m\} \subseteq \mathcal{V} \times \mathcal{V}$. An ordered pair (v_i, v_j) denotes the directed edge from node v_i to node v_j, where v_i is defined as initial node and v_j is defined as terminal node. A directed path of length s is a sequence of edges $(v_{i_0}, v_{i_1}), \ldots, (v_{i_{s-1}}, v_{i_s})$. A directed graph contains a directed *spanning tree* if there exists at least one node having directed paths connected to all other nodes. A directed graph is called strongly connected if and only if any two distinct nodes of $\mathcal{D}$ can be connected via a directed path; weakly connected if $\mathcal{D}$ is connected when viewed as a disoriented directed graph; quasi-strongly connected id $\mathcal{D}$ has a center from which any other node is reachable [18]. If a directed graph $\mathcal{D}$ is quasi-strongly connected, it has a spanning tree [20]. N_i, the neighbor set of node i, is defined as $N_i = \{v_j \in \mathcal{V} : (v_j, v_i) \in \mathcal{E}\}$. The adjacency matrix $A \in \mathbb{R}^{n\times n}$ of graph $\mathcal{D}$ indicates the vertex adjacency relationship, with entries $a_{ij} = 1$ if $(v_i, v_j) \in \mathcal{E}$, and $a_{ij} = 0$ otherwise. Let D be the $n \times n$ diagonal matrix of d_i's, where the degree d_i of each vertex i is given by $d_i = \sum_{j=1}^{n} a_{ij}$. The Laplacian matrix of G is a symmetric positive semi-definite matrix given by $L = D - A$. The $m \times n$ incidence matrix H and in-incidence matrix $H_{\bigodot}$ associated to directed graph $\mathcal{D}$ is defined the same as (1) and (2). With incidence matrix H and in-incidence matrix $H_{\bigodot}$, the Laplacian matrix L can also given by $L = H_{\bigodot}^T H$. The edge Laplacian matrix L_e can be given by $L_e = HH_{\bigodot}^T$.

For directed sensing topologies, the relative state vector can be constructed as:

$$z = Hx \tag{8}$$

where $z = [z_1, z_2, \cdots, z_m]^T \in \mathbb{R}^m$, with $z_r \in \mathbb{R}$ being the relative state over ϵ_r.

For an directed graph, we have the following lemma:

Lemma 2.3. *[18] If the underlying directed graph is quasi-strongly connected and associated with the edge Laplacian L_e, then there exits a symmetric positive definite matrix P satisfying the equation*

$$PL_e + L_e^T P = Q \geq 0 \tag{9}$$

where Q is a positive semi-definite matrix.

Remark 2.1. *For notation simplicity, we only consider one-dimensional case in this paper. However, it is easy to extend our results to higher dimensional spaces by using Kronecker multiplicity.*

3 Synchronized clock case under undirected graph

3.1 Problem formulation

We assume that each agent is only equipped with relative position sensors, e.g. sonar or ToF (time-of-flight) camera, to measure the relative states between its neighbours and itself, in its own local coordinate frame. We further assume that all agents share a global clock t, i.e. each agent in the multi-agent system (MAS) are activated simultaneously. The sensing topology is captured by a fixed, undirected and connected graph $\mathcal{G}$ with corresponding incidence matrix H, Laplacian matrix L and adjacency matrix A. For each edge ϵ_r connecting agent i and agent j, both agent i and agent j measure the relative state z_r continuously.

The MAS we study in this paper consists of n single integrators that are labelled from 1 to n. The n agents are connected by m edges (sensing link), labelled from 1 to m. Let $x_i(t) \in \mathbb{R}$ denote the state of agent i, $i = 1, 2, \ldots n$. The dynamics of agent i are described by

$$\dot{x}_i(t) = u_i(t), \quad i = 1, 2, \ldots, n, \tag{10}$$

where $u_i(t)$ is the control input. The sequence of event-triggered executions for edge ϵ_r is $t_{0_r} = 0, t_{1_r}, \ldots, t_{k_r}, \ldots$. At t_{k_r}, agent i and agent j linked by edge ϵ_r update their control input simultaneously. This synchronous controller updating phenomenon results from the fact that agents i and j share a global clock. We will provide detailed explanations about this phenomenon in the main result subsection. For agent i, which is one agent of the agent pair (i, j) linked by edge ϵ_r, the control input is designed as follows:

$$u_i(t) = \sum_{j \in N_i} (x_j(t_{k_r}) - x_i(t_{k_r})) \tag{11}$$

for $t \in [t_{k_r}, t_{k_r+1})$. We emphasize that only partial information $x_j(t_{k_r}) - x_i(t_{k_r})$ in the control input is updated at t_{k_r}. Moreover, by observing (35), we see that control input uses only relative information.

The key problem in event-triggered control is to determine the next trigger time t_{k_r+1}, which ensures the global control objective is achieved. In this section, we first design a basic edge-event-based trigger algorithm. Then to overcome the drawback that the basic algorithm can not exclude Zeno behaviour completely, an improved algorithm to achieve Zeno-free triggers.

3.2 Main result

3.2.1 Basic algorithm

We first introduce a time-varying error $e_r(t)$. For time $t \in [t_{k_r}, t_{k_r+1})$, the relative state measurement error for edge ϵ_r is defined as

$$e_r(t) = z_r(t_{k_r}) - z_r(t), \;\; r = 1, \ldots, m \tag{12}$$

We note that $e_r(t)$ is actually calculated by agents i and j linked by ϵ_r separately using their own on-board processors. However, since agents i and j share a global clock, the values of $\|e_r(t)\|$ calculated inside their processors are identical. In the design of basic edge event algorithm, the strategy in [21] is used. That is, an edge event occurs when a given trigger function is equal to zero. The trigger function is proposed as

$$f(e_r(t), z_r(t)) = \|e_r(t)\| - \beta_r \|z_r(t)\| \tag{13}$$

with $\beta_r > 0$. Note that agents i and j linked by ϵ_r share the same observations of $\|e_r(t)\|$ and $\|z_r(t)\|$, which means equation (37) calculated inside both the agents' processors reach zero at the same time. This is the reason that the controller updates for agents i, j are synchronous, presented in our problem formulation. We call (37) the edge trigger function. Furthermore, every time an edge event is triggered, and in accordance with its definition (36), the measurement error $e_r(t)$ is reset to zero. Furthermore, it is obvious that the trigger function only use relative information. Since both input and trigger condition use only relative information, we conclude that the knowledge of a global coordinate frame is not required in our framework.

Theorem 1. *Consider a multi-agent system where each agent's dynamics are described by* (34) *with control input* (35)*, trigger function* (37)*. If* β_r *satisfies* $0 < \beta_r < \frac{\lambda_2(L)}{\|H\|^2}$*, then*

- *(Average consensus) All agents' states will converge to their initial average* $\sum_{i=1}^{n} x_i(0)/n$.

- *(No Zeno behaviour for at least one edge) At any time $t > 0$, there exists at least one edge that does not exhibit Zeno behaviour.*

Proof. At the beginning of the proof, we clarify that the analysis requires the knowledge of a global coordinate frame, i.e. the relative state vector z (4) is defined according to a global coordinate frame. However, the implementation of the algorithm only requires the knowledge of agent's own local coordinate frame. We now prove the the first statement. It is well-known that the compact form of continuous-time consensus dynamic is constructed $\dot{x} = -Lx = -H^T z$. Following this construction, the compact form of (35) can be written as

$$u(t) = -H^T \begin{bmatrix} z_1(t_{k_1}) \\ z_2(t_{k_2}) \\ \vdots \\ z_m(t_{k_m}) \end{bmatrix} \tag{14}$$

where $k_r = \arg\max_{k_r \in \mathbb{N}} \{t_{k_r} | t_{k_r} \leq t\}, r = 1, \ldots, m$. By substituting the edge measurement error (36), the compact form of the consensus dynamic can be written as

$$\dot{x}(t) = -H^T z(t) - H^T e(t) \tag{15}$$

where $z(t) = [z_1(t), z_2(t), \ldots, z_m(t)]^T$ and $e(t) = [e_1(t), e_2(t), \ldots, e_m(t)]^T$.

Consider the following Lyapunov function

$$V(t) = \frac{1}{2} z(t)^T z(t). \tag{16}$$

The time derivative of the Lyapunov function (16) along (15) is

$$\begin{aligned} \dot{V}(t) &= z(t)^T \dot{z}(t) = z(t)^T H \dot{x}(t) \\ &= -z(t)^T H H^T z(t) - z(t)^T H H^T e(t). \end{aligned}$$

From Lemma 2.2, we further obtain

$$\begin{aligned} \dot{V}(t) &\leq -\lambda_2(L) \|z(t)\|^2 + \|H\|^2 \|e(t)\| \|z(t)\| \\ &\leq -\left(\lambda_2(L) \|z(t)\| - \|H\|^2 \|e(t)\|\right) \|z(t)\|. \end{aligned} \tag{17}$$

Note that the edge measurement error $e_r(t)$ is reset to zero as soon as the trigger function (37) is equal to zero, which means $\|e_r(t)\| \leq \beta_r \|z_r(t)\|$ holds through-out the evolution of

the corresponding $z_r(t)$. Define $\beta_{\max} = \max\{\beta_r : r = 1, 2, \ldots, m\}$, and it is obvious that the inequality $\|e(t)\| \leq \beta_{\max}\|z(t)\|$ also holds. So we further have

$$\dot{V}(t) \leq -(\lambda_2(L) - \beta_{\max}\|H\|^2)\|z(t)\|^2. \tag{18}$$

If we enforce the value of β_r to satisfy $\beta_r \in (0, \frac{\lambda_2(L)}{\|H\|^2})$, $\dot{V}(t) < 0$ can be guaranteed, which means consensus can be reached as $t \to \infty$.

The above analysis shows that the system (**??**) will converge to a consensus point. Now we prove that the consensus value is their initial average. Define average variable

$$\bar{x}(t) = \frac{1}{n}\sum_{i=1}^{n} x_i(t).$$

The time derivative of $\bar{x}(t)$ is

$$\begin{aligned}\dot{\bar{x}}(t) &= \frac{1}{n}\sum_{i=1}^{n}\dot{x}_i(t) = \frac{1}{n}\sum_{i=1}^{n}u_i(t)\\ &= \frac{1}{n}\sum_{i=1}^{n}\sum_{j\in N_i}\left(x_j(t_{k_r}) - x_i(t_{k_r})\right).\end{aligned}$$

Since $j \in N_i$ represents the adjacency relation between agent i and agent j, the above equation can be reformulated as

$$\dot{\bar{x}}(t) = \frac{1}{n}\sum_{i=1}^{n}\sum_{j=1}^{n} a_{ij}\left(x_j(t_{k_r}) - x_i(t_{k_r})\right).$$

Applying the symmetric property of undirected graph shows:

$$\begin{aligned}\dot{\bar{x}}(t) &= \frac{1}{2n}\sum_{i=1}^{n}\sum_{j=1}^{n} a_{ij}\left(x_j(t_{k_r}) - x_i(t_{k_r})\right)\\ &\quad + \frac{1}{2n}\sum_{j=1}^{n}\sum_{i=1}^{n} a_{ji}\left(x_i(t_{k_r}) - x_j(t_{k_r})\right)\\ &= \frac{1}{2n}\sum_{i=1}^{n}\sum_{j=1}^{n}\Big(a_{ij}(x_j(t_{k_r}) - x_i(t_{k_r}))\\ &\qquad\qquad + a_{ji}(x_i(t_{k_r}) - x_i(t_{k_r}))\Big)\\ &= 0,\end{aligned} \tag{19}$$

which means the average state $\dot{\bar{x}}(t)$ remains a constant. Note that the previous analysis has shown that the consensus can be reached, so it is obvious that the final consensus value is their initial average.

For the second statement, it is noted that there holds $\|e_r(t)\| \leq \|e(t)\|$ for any r. Also note that at any time t, there exists an edge $r*$ such that $\|z_{r*}(t)\|^2 \geq \frac{1}{m}\|z(t)\|^2$. Then one obtains

$$\frac{\|e_{r*}(t)\|}{\|z_{r*}(t)\|} \leq \sqrt{m}\frac{\|e(t)\|}{\|z(t)\|}.$$

Following the similar argument proposed in [5] (see its proof of Theorem 4), we focus on the dynamic of $\|e(t)\|/\|z(t)\|$ and its time derivative $d(\|e(t)\|/\|z(t))\|)/dt$, where a strictly positive lower bound of inter-edge-event interval can be obtained. This guarantees the second statement. □

3.2.2 Zeno-free algorithm

In order to avoid Zeno behaviour for *all* edges, we propose an alternative algorithm by following the idea proposed in [11]. The next event time for edge ϵ_r is determined by

$$t_{k_r+1} = t_{k_r} + \max\{\tau_{k_r}, b_r\} \tag{20}$$

where b_r is a strictly positive real number and τ_{k_r} is determined by the trigger function (37), described by:

$$\tau_{k_r} = \inf_{t>t_{k_r}} \{t - t_{k_r} | f(e_r(t), z_r(t)) = 0\}. \tag{21}$$

Remark 3.1. *We note that this approach can eliminate Zeno behaviour since the inter-edge-event time for edge ϵ_r is lower bounded by a strictly positive number b_r. However, in the Zeno time for edge ϵ_r, both two connected agent i and j have to calculate the inter-edge-event time with high frequency, causing great burden to processors of agents. The trade-off for the inter-edge-event time should be concerned.*

Theorem 2. *Consider a multi-agent system where each agent's dynamics are described by* (34) *with control input* (35) *and the edge trigger condition* (20)*. Let η_1 and η_2 be positive real numbers satisfying $\eta_1 + \eta_2 < 1$. If $\beta_r \leq \eta_1(\lambda_2(L)/\|H\|^2)$ for all edges, b_r is strictly positive and satisfies*

$$b_r \leq \frac{\eta_2\lambda_2(L)}{\|H\|^2\left(\sqrt{m}\|H\|^2 + \eta_2\lambda_2(L)\right)}. \tag{22}$$

- *(Average consensus) All agents' states converge to their initial average.*
- *(Zeno-free triggers) At any time $t > 0$, no edge will exhibit Zeno behaviour.*

Proof. We continue using the Lyapunov function (**??**) and omit several steps of the time derivative calculation. According to equation (17), we obtain

$$\begin{aligned}\dot{V}(t) &\leq -\left(\lambda_2(L)\|z(t)\| - \|H\|^2\|e(t)\|\right)\|z(t)\| \\ &= -\left(\lambda_2(L)\sqrt{\sum_{r=1}^{m}\|z_r(t)\|^2}\right. \\ &\qquad \left. -\|H\|^2\sqrt{\sum_{r=1}^{m}\|e_r(t)\|^2}\right)\|z(t)\|.\end{aligned} \tag{23}$$

If we can guarantee that

$$\sum_{r=1}^{m}\|e_r(t)\|^2 \leq \eta^2\left(\frac{\lambda_2(L)}{\|H\|^2}\right)^2\sum_{r=1}^{m}\|z_r(t)\|^2 \tag{24}$$

with $\eta \in (0,1)$, then it yields

$$\dot{V}(t) \leq -\left((1-\eta)\lambda_2(L)\sqrt{\sum_{r=1}^{m}\|z_r(t)\|^2}\right)\|z(t)\| < 0. \tag{25}$$

According to (20), we know that at any time $t > 0$, the determination of inter-edge-event time of edge ϵ_r is either by τ_{k_r} or b_r. Let $S_1(t)$ and $S_2(t)$ be the edge sets consisting of edges whose next inter-edge-event time at t is τ_{k_r} and b_r, respectively. Then it is obvious that $S_1(t)\bigcup S_2(t) = \{\epsilon_1, \ldots, \epsilon_m\}$ and $S_1(t)\bigcap S_2(t) = \emptyset$. To guarantee (51), we further propose the following two conditions:

$$\begin{aligned}\sum_{\epsilon_r\in S_1(t)}\|e_r(t)\|^2 &\leq \eta_1^2\left(\frac{\lambda_2(L)}{\|H\|^2}\right)^2\sum_{\epsilon_r\in S_1(t)}\|z_r(t)\|^2 \\ &\leq \eta_1^2\left(\frac{\lambda_2(L)}{\|H\|^2}\right)^2\sum_{r=1}^{m}\|z_r(t)\|^2\end{aligned} \tag{26}$$

and

$$\begin{aligned}\sum_{\epsilon_r\in S_2(t)}\|e_r(t)\|^2 &\leq \eta_2^2\left(\frac{\lambda_2(L)}{\|H\|^2}\right)^2\sum_{\epsilon_r\in S_2(t)}\|z_r(t)\|^2 \\ &\leq \eta_2^2\left(\frac{\lambda_2(L)}{\|H\|^2}\right)^2\sum_{r=1}^{m}\|z_r(t)\|^2\end{aligned} \tag{27}$$

where η_1 and η_2 are strictly positive real numbers under the condition that $\eta_1+\eta_2 = \eta < 1$. For each edge in $S_1(t)$, if we let $\beta_r \leq \eta_1(\lambda_2(L)/\|H\|^2)$, then condition (52) will holds for all t. For condition (53), if we can guarantee

$$\|e_r(t)\|^2 \leq \frac{\eta_2^2}{m}\left(\frac{\lambda_2(L)}{\|H\|^2}\right)^2\sum_{j=1}^{m}\|z_j(t)\|^2, \tag{28}$$

then condition (53) will holds. Let $\zeta = \frac{\eta_2^2}{m}\left(\frac{\lambda_2(L)}{\|H\|^2}\right)^2$, (54) can be rewritten as

$$\|e_r(t)\| \leq \sqrt{\zeta}\|z(t)\|. \tag{29}$$

Since ζ is strictly positive, the evolution time of $\|e_r(t)\|/\|z(t)\|$ from 0 to $\sqrt{\zeta}$ is strictly positive (because $\|z(t)\| \neq 0$, $\|e_r(t)\|$ evolutes from 0 at t_{k_r}). By finding an upper bound B_r of this evolution time, we can determine a strictly positive time $b_r \leq B_r$. Then condition (55) can always be guaranteed if the evolution time of $\|e_r(t)\|/\|z(t)\|$ is b_r. To find B_r, we first estimate the time derivative of $\|e_r(t)\|/\|z(t)\|$:

$$\begin{aligned} \frac{d}{dt}\frac{\|e_r\|}{\|z\|} &= \frac{e_r^T\dot{e}_r}{\|e_r\|\|z\|} - \frac{\|e_r\|z^T\dot{z}}{\|z\|^3} \\ &\leq \frac{\|\dot{e}_r\|}{\|z\|} + \frac{\|e_r\|}{\|z\|}\frac{\|\dot{z}\|}{\|z\|}. \end{aligned} \tag{30}$$

According to (36), one can deduce that $\dot{e}_r = -\dot{z}_r$. So it is obvious that

$$\begin{aligned} \frac{d}{dt}\frac{\|e_r\|}{\|z\|} &\leq \frac{\|\dot{z}\|}{\|z\|} + \frac{\|e\|}{\|z\|}\frac{\|\dot{z}\|}{\|z\|} \\ &= (1+\frac{\|e\|}{\|z\|})\frac{\|\dot{z}\|}{\|z\|} = (1+\frac{\|e\|}{\|z\|})\frac{\|H\dot{x}\|}{\|z\|} \\ &= (1+\frac{\|e\|}{\|z\|})\frac{\|HH^T\left(z(t)+e(t)\right)\|}{\|z\|} \\ &\leq \|HH^T\|(1+\frac{\|e\|}{\|z\|})^2 = \|H\|^2(1+\frac{\|e\|}{\|z\|})^2. \end{aligned} \tag{31}$$

Thus it holds that

$$\frac{d}{dt}\frac{\|e_r\|}{\|z\|} \leq \|H\|^2(1+\frac{\|e\|}{\|z\|})^2.$$

Similar time derivative of $\|e(t)\|/\|z(t)\|$ yields

$$\frac{d}{dt}\frac{\|e\|}{\|z\|} \leq \|H\|^2(1+\frac{\|e\|}{\|z\|})^2.$$

It is noticed that $\|e\|/\|z\|$ always upper bounds $\|e_r\|/\|z\|$ and both of them are non-negative. Now we conclude that $\|e_r\|/\|z\| < g(t, g_0)$, where $g(t, g_0)$ is the solution of $\dot{g}(t) = \|H\|^2(1+g(t))^2$, $g_0 = 0$. Thus the lower bound of evolution time of $\|e_r\|/\|z\|$ from

0 to $\sqrt{\zeta}$ is

$$\begin{aligned} B_r &= \frac{\sqrt{\zeta}}{\|H\|^2(1+\sqrt{\zeta})} \\ &= \frac{\sqrt{\frac{\eta_2^2}{m}\left(\frac{\lambda_2(L)}{\|H\|^2}\right)^2}}{\|H\|^2\left(1+\sqrt{\frac{\eta_2^2}{m}\left(\frac{\lambda_2(L)}{\|H\|^2}\right)^2}\right)} \\ &= \frac{\eta_2\lambda_2(L)}{\|H\|^2\left(\sqrt{m}\|H\|^2+\eta_2\lambda_2(L)\right)}. \end{aligned} \tag{32}$$

We can choose a strictly positive real time b_r which is satisfied with $b_r \leq B_r$ to guarantee (53) for each edge in $S_2(t)$. Since b_r is strictly positive, it is straightforward to conclude that Zeno behaviour is excluded for each edge. Moreover, since condition (51) can be ensured, we also conclude that consensus can be reached. Note that (19) still holds in the Zeno-free algorithm, which means the final consensus value remains to be the initial average. □

3.3 Simulation

The MAS considered in the simulation consists of 5 agents. The sensing topology is described by Fig. 3 whose incidence matrix is chosen as

$$H = \begin{bmatrix} -1 & 1 & 0 & 0 & 0 \\ 0 & -1 & 1 & 0 & 0 \\ -1 & 0 & 1 & 0 & 0 \\ 0 & 0 & 1 & 0 & -1 \\ 0 & 0 & -1 & 1 & 0 \\ 0 & 0 & 0 & -1 & 1 \\ 1 & 0 & 0 & 0 & -1 \\ -1 & 0 & 0 & 1 & 0 \end{bmatrix} \tag{33}$$

The initial states for all agents are set as $x_1(0) = -3.2$, $x_2(0) = 2.1$, $x_3(0) = -2.7$, $x_4(0) = 4.3$ and $x_5(0) = 1.6$. The parameter β_r for the basic edge-event algorithm is selected as $\beta_r = 0.34$ for each edge trigger function. In the Zeno-free edge-event algorithm, the parameter η_1 and η_2 are chosen as $\eta_1 = 0.85$ and $\eta_2 = 0.14$, then we also set $\beta_r = 0.34$ for the trigger function (21) in the Zeno-free trigger algorithm. The minimal inter-edge-event time b_r is chosen as $b_r = 0.0039s$, which satisfies the condition (22).

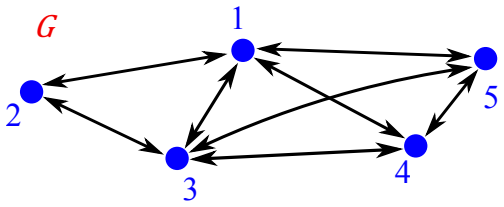

Figure 3: Undirected graph topology.

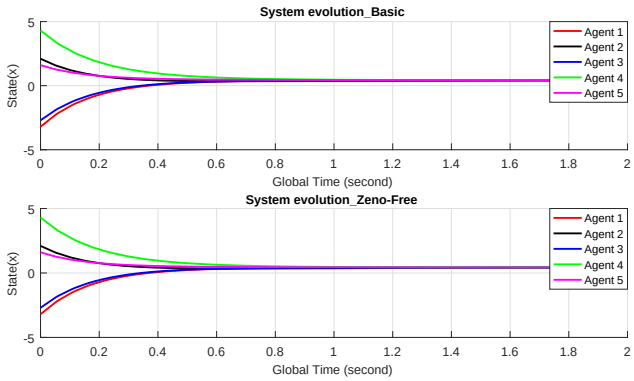

Figure 4: Comparison of state trajectories.

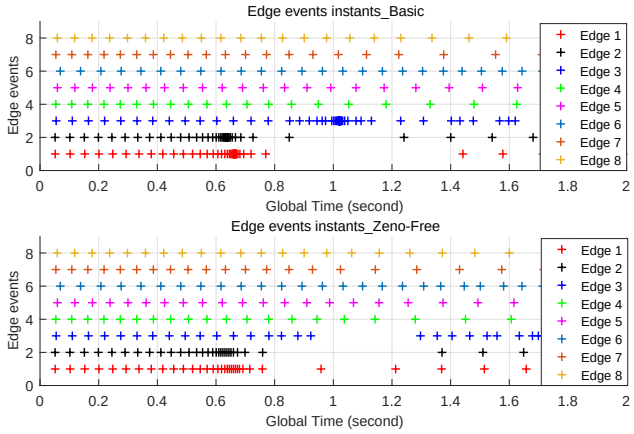

Figure 5: Comparison of edge event times.

The state trajectories and trigger performance for both the basic algorithm and the Zeno-free algorithm are compared in Fig. 4 and 5, respectively. Table 1 compares the edge event numbers for each edge between the the basic algorithm and the Zeno-free algorithm. Note that the minimum inter-edge-event time interval we observed in the simulation of the basic algorithm is $1 \times 10^{-6} s$, which is the numerical accuracy we set in Matlab. This dense triggering behaviour is observed when the state term $z_r(t)$ crosses zero, which supports

Table 1: Comparison of numbers of edge events.

Number of edge	Basic	Zeno-free
Edge 1	85	39
Edge 2	87	41
Edge 3	98	70
Edge 4	24	24
Edge 5	26	26
Edge 6	31	31
Edge 7	25	25
Edge 8	26	26
Total	402	282

the analysis of Zeno behaviour in [14] (see its Remark 2). The minimum inter-edge-event time interval observed in the simulation of the Zeno-free algorithm is $0.0039s$, which corresponds to the value of b_r calculated in the last paragraph.

Remark 3.2. *Since the choice of β_r is quite conservative, depending on the global information of sensing topology. i.e. $\|H\|$ and $\lambda_2(L)$, an alternative Lyapunov defined by group disagreement has been proposed to relax the limitation of β_r for future work.*

4 Synchronized clock case under directed graph

4.1 Problem formulation

In this section, we assume that continuous local relative information is available to each agent and all agents share a global clock t. The sensing topology is captured by a fixed, directed and quasi-strongly connected graph $\mathbb{D}$ with associated incidence matrix H, in-incidence matrix $H_{\bigodot}$, Laplacian matrix L, edge Laplacian matrix. For each information link ϵ_r connecting agent i and agent j, the terminal agent can measure the relative state to terminal agent.

The MAS we study in this report consists of n signal integrators that are labelled from 1 to n. The n agents are connected by m edges (sensing link), labelled from 1 to m. Let $x_i(t) \in \mathbb{R}$ denote the state of agent i, $i = 1, 2, \ldots, n$. The dynamics of agent i are

described by

$$\dot{x}_i(t) = u_i(t), \;\; i = 1, 2, \ldots, n, \tag{34}$$

where $u_i(t)$ is the control input. The sequence of event-triggered executions for edge ϵ_r is $t_{0_r} = 0, t_{1_r}, \ldots, t_{k_r}, \ldots$. At t_{k_r}, only the terminal agent of edge ϵ_r updates its control protocol. For agent i, which is the terminal agent of the agent pair (j, i) linked by edge ϵ_r, the control protocol is designed as follows:

$$u_i(t) = \sum_{j=1}^{n} (h_{\odot})_{ji} \left(x_j(t_{k_r}) - x_i(t_{k_r}) \right) \tag{35}$$

for $t \in [t_{k_r}, t_{k_r+1})$. We emphasize that only partial information $x_j(t_{k_r}) - x_i(t_{k_r})$ in the control protocol is updated at t_{k_r}. Moreover, by observing (35), we see that control protocol uses only relative information.

The key problem in event-triggered control is to determine the next trigger time t_{k_r+1}, which ensures the global control objective is achieved. In this section, we first design a basic edge-event-based trigger algorithm. Then to overcome the drawback that the basic algorithm can not exclude Zeno behaviour completely, an improved algorithm to achieve Zeno-free triggers.

4.2 Main result

4.2.1 Basic trigger scheme

We first introduce a time-varying error $e_r(t)$. For time $t \in [t_{k_r}, t_{k_r+1})$, the relative state measurement error for edge ϵ_r is defined as

$$e_r(t) = z_r(t_{k_r}) - z_r(t), \;\; r = 1, \ldots, m \tag{36}$$

We note that $e_r(t)$ is only calculated by the initial agent i of edge ϵ_r, where agent j is the terminal agent. In the design of basic edge event algorithm, the strategy in [21] is used. That is, an edge event occurs when a given trigger function reaches zero. The trigger function is proposed as

$$f(e_r(t), z_r(t)) = \|e_r(t)\| - \beta_r \|z_r(t)\| \tag{37}$$

with $\beta_r > 0$. Furthermore, every time an edge event is triggered, and in accordance with its definition (36), the measurement error $e_r(t)$ is reset to zero. What's more, it is

obvious that the trigger function only use relative information. Since both protocol and trigger condition use only relative information, we conclude that the knowledge of a global coordinate frame is not required in our framework.

Theorem 3. *Consider a multi-agent system where each agent's dynamics are described by* (34) *with control protocol* (35)*, trigger function* (37)*. Suppose the sensing topologies* $\mathcal{D}$ *are quasi-strongly connected. For any given positive semi-definite matrix* Q*. If* β_r *satisfies* $0 < \beta_r < \frac{\lambda_2(Q)}{\|Q\|}$*, then*

- *(Consensus) All agents' states will reach consensus.*
- *(No Zeno behaviour for at least one edge) At any time* $t > 0$*, there exists at least one edge that does not exhibit Zeno behaviour.*

Proof. At the beginning of the proof, we clarify that the analysis requires the knowledge of a global coordinate frame, i.e. the relative state vector z (4) is defined according to a global coordinate frame. However, the implementation of the algorithm only requires the knowledge of agent's own local coordinate frame. We now prove the the first statement. It is well-known that the compact form of continuous-time consensus dynamic is constructed $\dot{x} = -Lx = -H_{\bigodot}^T z$. Following this construction, the compact form of (35) can be written as

$$u(t) = -H_{\bigodot}^T \begin{bmatrix} z_1(t_{k_1}) \\ z_2(t_{k_2}) \\ \vdots \\ z_m(t_{k_m}) \end{bmatrix} \tag{38}$$

where $k_r = \arg\max_{k_r \in \mathbb{N}} \{t_{k_r} | t_{k_r} \leq t\}, r = 1, \ldots, m$. By substituting the edge measurement error (36), the compact form of the consensus dynamic can be written as

$$\dot{x}(t) = -H_{\bigodot}^T z(t) - H_{\bigodot}^T e(t) \tag{39}$$

where $z(t) = [z_1(t), z_2(t), \ldots, z_m(t)]^T$ and $e(t) = [e_1(t), e_2(t), \ldots, e_m(t)]^T$. Left multiplying an in-incidence matrix H for both side of (39), we can obtained so called edge dynamics of system, that is

$$\begin{aligned} \dot{z}(t) &= -HH_{\bigodot}^T z(t) - HH_{\bigodot}^T e(t) \\ &= -L_e z(t) - L_e e(t) \end{aligned} \tag{40}$$

Consider the following Lyapunov function,

$$V(t) = z^T(t)Pz(t), \tag{41}$$

where P is a symmetric positive definite matrix calculated by lemma 2.3.

The time derivative of the Lyapunov function (41) alone (39) is

$$\begin{aligned}
\dot{V}(t) &= \dot{z}^T(t)Pz(t) + z^T(t)P\dot{z}(t) \\
&= \left(-L_e z(t) - L_e e(t)\right)^T Pz(t) + z^T(t)P\left(-L_e z(t) - L_e e(t)\right) \\
&= \left(-z^T(t)L_e^T - e^T(t)L_e^T\right)Pz(t) + z^T(t)P\left(-L_e z(t) - L_e e(t)\right) \\
&= -z^T(t)L_e^T Pz(t) - e^T(t)L_e^T Pz(t) - z^T(t)PL_e z(t) - z^T(t)PL_e e(t) \\
&= -z^T(t)\left(L_e^T P + PL_e\right)z(t) - \frac{1}{2}z^T(t)\left(L_e^T P + PL_e\right)e(t)
\end{aligned} \tag{42}$$

From lemma 2.3, we can further obtain

$$\begin{aligned}
\dot{V}(t) &\leq -\lambda_2(Q)\|z(t)\|^2 + \|z(t)\|\|L_e^T P + PL_e\|\|e(t)\| \\
&\leq -\left(\lambda_2(Q)\|z(t)\| - \|Q\|\|e(t)\|\right)\|z(t)\|
\end{aligned} \tag{43}$$

Note that the edge measurement error $e_r(t)$ is reset to zero once the trigger function (37) reaches to zero, which indicates that $\|e_r(t)\| \leq \beta_r\|z_r(t)\|$ holds through the evolution of the associated edge $z_r(t)$. Let $\beta_{\max} = \max\{\beta_r : r = 1, 2, \ldots, m\}$, and the inequality $\|e(t)\| \leq \beta_{\max}\|z(t)\|$ also holds. Thus we can further obtain that

$$\dot{V}(t) \leq -\left(\lambda_2(Q) - \beta_{\max}\|Q\|\right)\|z(t)\|^2 \tag{44}$$

If the value of β_r is enforced to satisfied $\beta_r \in (0, \frac{\lambda_2(Q)}{\|Q\|})$, $\dot{V}(t) \leq 0$ can be guaranteed, indicating that consensus can be reached as $t \to \infty$.

Now we turn to the second statement. Note that there holds $\|e_r(t)\| \leq \|e(t)\|$ for any r. Also note that at any time t, there exists an edge $r*$ such that $\|z_{r*}(t)\|^2 \geq \frac{1}{m}\|z(t)\|^2$. Then one yields

$$\frac{\|e_{r*}(t)\|}{\|z_{r*}(t)\|} \leq \sqrt{m}\frac{\|e(t)\|}{\|z(t)\|} \tag{45}$$

Following the similar argument proposed in [5] (see the proof of Theorem 4), we focus on the dynamic of $\|e(t)\|/\|z(t)\|$ and its time derivative $d(\|e(t)\|/\|z(t))\|)/dt$, where a strictly positive lower bound of inter-edge-event interval can be obtained. This guarantees the second statement. □

4.2.2 Zeno-free trigger scheme

In order to avoid Zeno behaviour for *all* edges, an alternative algorithm is proposed. The next event time for edge ϵ_r is determined by

$$t_{k_r+1} = t_{k_r} + \max\{\tau_{k_r}, b_r\}, \tag{46}$$

where b_r is a strictly real number and τ_{k_r} is determined by the trigger function (37), which is described by:

$$\tau_{k_r} = \inf_{t>t_{k_r}} \{t - t_{k_r} | f(e_r(t), z_r(t)) = 0\}. \tag{47}$$

Theorem 4. *Consider a multi-agent system where each agent's dynamics are described by* (34) *with control protocol* (35)*, and edge trigger condition* (46)*. Suppose the sensing topologies $\mathcal{D}$ are quasi-strongly connected. Suppose the sensing topologies $\mathcal{D}$ are quasi-strongly connected. For any given positive semi-definite matrix Q. Let η_1 and η_2 be positive real numbers satisfying $\eta_1 + \eta_2 < 1$. If $\beta_r \leq \eta_1(\lambda_2(Q)/\|Q\|)$ for all edges, b_r is strictly positive and satisfies*

$$b_r \leq \frac{\eta_2 \lambda_2(Q)}{\|L_e\| \left(\sqrt{m}\|Q\| + \eta_2 \lambda_2(Q)\right)}. \tag{48}$$

- *(Consensus) All agents' states will reach consensus.*
- *(Zeno free triggering) At any time $t > 0$, no edge will exhibit Zeno behaviour.*

Proof. We continue using the Lyapunov function (41) and omit several steps of the time derivative calculation. According to equation (43), we obtain

$$\begin{aligned} \dot{V}(t) &\leq -\left(\lambda_2(Q)\|z(t)\| - \|Q\|\|e(t)\|\right)\|z(t)\| \\ &= -\left(\lambda_2(Q)\sqrt{\sum_{r=1}^{m}\|z_r(t)\|^2}\right. \\ &\qquad \left. -\|Q\|\sqrt{\sum_{r=1}^{m}\|e_r(t)\|^2}\right)\|z(t)\|. \end{aligned} \tag{49}$$

If we can guarantee that

$$\sum_{r=1}^{m}\|e_r(t)\|^2 \leq \eta^2 \left(\frac{\lambda_2(Q)}{\|Q\|}\right)^2 \sum_{r=1}^{m}\|z_r(t)\|^2 \tag{50}$$

with $\eta \in (0,1)$, then it yields

$$\dot{V}(t) \leq -\left((1-\eta)\lambda_2(Q)\sqrt{\sum_{r=1}^{m}\|z_r(t)\|^2}\right)\|z(t)\| < 0. \tag{51}$$

According to (46), we know that at any time $t > 0$, the determination of inter-edge-event time of edge ϵ_r is either by τ_{k_r} or b_r. Let $S_1(t)$ and $S_2(t)$ be the edge sets consisting of edges whose next inter-edge-event time at t is τ_{k_r} and b_r, respectively. Then it is obvious that $S_1(t)\bigcup S_2(t) = \{\epsilon_1, \ldots, \epsilon_m\}$ and $S_1(t)\bigcap S_2(t) = \emptyset$. To guarantee (51), we further propose the following two conditions:

$$\begin{aligned}\sum_{\epsilon_r \in S_1(t)}\|e_r(t)\|^2 &\leq \eta_1^2\left(\frac{\lambda_2(Q)}{\|Q\|}\right)^2\sum_{\epsilon_r \in S_1(t)}\|z_r(t)\|^2 \\ &\leq \eta_1^2\left(\frac{\lambda_2(Q)}{\|Q\|}\right)^2\sum_{r=1}^{m}\|z_r(t)\|^2\end{aligned} \tag{52}$$

and

$$\begin{aligned}\sum_{\epsilon_r \in S_2(t)}\|e_r(t)\|^2 &\leq \eta_2^2\left(\frac{\lambda_2(Q)}{\|Q\|}\right)^2\sum_{\epsilon_r \in S_2(t)}\|z_r(t)\|^2 \\ &\leq \eta_2^2\left(\frac{\lambda_2(Q)}{\|Q\|}\right)^2\sum_{r=1}^{m}\|z_r(t)\|^2\end{aligned} \tag{53}$$

where η_1 and η_2 are strictly positive real numbers under the condition that $\eta_1 + \eta_2 = \eta < 1$. For each edge in $S_1(t)$, if we let $\beta_r \leq \eta_1(\lambda_2(Q)/\|Q\|)$, then condition (52) will holds for all t. For condition (53), if we can guarantee

$$\|e_r(t)\|^2 \leq \frac{\eta_2^2}{m}\left(\frac{\lambda_2(Q)}{\|Q\|}\right)^2\sum_{j=1}^{m}\|z_j(t)\|^2, \tag{54}$$

then condition (53) will holds. Let $\zeta = \frac{\eta_2^2}{m}\left(\frac{\lambda_2(Q)}{\|Q\|}\right)^2$, (54) can be rewritten as

$$\|e_r(t)\| \leq \sqrt{\zeta}\|z(t)\|. \tag{55}$$

Since ζ is strictly positive, the evolution time of $\|e_r(t)\|/\|z(t)\|$ from 0 to $\sqrt{\zeta}$ is strictly positive (because $\|z(t)\| \neq 0$, $\|e_r(t)\|$ evolutes from 0 at t_{k_r}). By finding an upper bound B_r of this evolution time, we can determine a strictly positive time $b_r \leq B_r$. Then condition (55) can always be guaranteed if the evolution time of $\|e_r(t)\|/\|z(t)\|$ is b_r. To

find B_r, we first estimate the time derivative of $\|e_r(t)\|/\|z(t)\|$:

$$\begin{aligned}\frac{d}{dt}\frac{\|e_r\|}{\|z\|} &= \frac{e_r^T\dot{e}_r}{\|e_r\|\|z\|} - \frac{\|e_r\|z^T\dot{z}}{\|z\|^3} \\ &\leq \frac{\|\dot{e}_r\|}{\|z\|} + \frac{\|e_r\|}{\|z\|}\frac{\|\dot{z}\|}{\|z\|} \\ &\leq \frac{\|\dot{z}\|}{\|z\|} + \frac{\|e\|}{\|z\|}\frac{\|\dot{z}\|}{\|z\|}.\end{aligned} \tag{56}$$

According to (36), one can deduce that $\dot{e}_r = -\dot{z}_r$. So it is obvious that

$$\begin{aligned}\frac{d}{dt}\frac{\|e_r\|}{\|z\|} &\leq \frac{\|\dot{z}\|}{\|z\|} + \frac{\|e\|}{\|z\|}\frac{\|\dot{z}\|}{\|z\|} \\ &= (1+\frac{\|e\|}{\|z\|})\frac{\|\dot{z}\|}{\|z\|} = (1+\frac{\|e\|}{\|z\|})\frac{\|H\dot{x}\|}{\|z\|} \\ &= (1+\frac{\|e\|}{\|z\|})\frac{\|L_e\left(z(t)+e(t)\right)\|}{\|z\|} \\ &\leq \|L_e\|(1+\frac{\|e\|}{\|z\|})^2.\end{aligned} \tag{57}$$

Thus it holds that

$$\frac{d}{dt}\frac{\|e_r\|}{\|z\|} \leq \|L_e\|(1+\frac{\|e\|}{\|z\|})^2.$$

Similar time derivative of $\|e(t)\|/\|z(t)\|$ yields

$$\frac{d}{dt}\frac{\|e\|}{\|z\|} \leq \|L_e\|(1+\frac{\|e\|}{\|z\|})^2.$$

It is noticed that $\|e\|/\|z\|$ always upper bounds $\|e_r\|/\|z\|$ and both of them are non-negative. Now we conclude that $\|e_r\|/\|z\| < g(t, g_0)$, where $g(t, g_0)$ is the solution of $\dot{g}(t) = \|H\|^2(1+g(t))^2$, $g_0 = 0$. Thus the lower bound of evolution time of $\|e_r\|/\|z\|$ from 0 to $\sqrt{\zeta}$ is

$$\begin{aligned}B_r &= \frac{\sqrt{\zeta}}{\|L_e\|(1+\sqrt{\zeta})} \\ &= \frac{\sqrt{\frac{\eta_2^2}{m}\left(\frac{\lambda_2(Q)}{\|Q\|}\right)^2}}{\|L_e\|\left(1+\sqrt{\frac{\eta_2^2}{m}\left(\frac{\lambda_2(Q)}{\|Q\|}\right)^2}\right)} \\ &= \frac{\eta_2\lambda_2(Q)}{\|L_e\|\left(\sqrt{m}\|Q\|+\eta_2\lambda_2(Q)\right)}.\end{aligned} \tag{58}$$

We can choose a strictly positive real time b_r which is satisfied with $b_r \leq B_r$ to guarantee (53) for each edge in $S_2(t)$. Since b_r is strictly positive, it is straightforward to conclude that Zeno behaviour is excluded for each edge. Moreover, since condition (51) can be ensured, we also conclude that consensus can be reached. □

4.3 Simulation

The MAS considered in the simulation consists of 5 agents. The sensing topology is described by Fig. 6 whose incidence matrix is chosen as

$$H = \begin{bmatrix} -1 & 1 & 0 & 0 & 0 \\ 0 & 1 & 0 & 0 & -1 \\ 0 & -1 & 0 & 1 & 0 \\ 0 & -1 & 1 & 0 & 0 \\ 0 & 0 & 1 & -1 & 0 \\ 0 & 0 & -1 & 0 & 1 \end{bmatrix} \tag{59}$$

The initial states for all agents are set as $x_1(0) = -3.5$, $x_2(0) = 4.1$, $x_3(0) = 2.7$, $x_4(0) = -4.3$ and $x_5(0) = 0.6$. The positive semi-definite matrix Q is selected as

$$Q = \begin{bmatrix} 1 & 0 & 0 & 0 & 0 & 0 \\ 0 & 1 & 0 & 0 & 0 & 0 \\ 0 & 0 & 1 & 0 & 0 & 0 \\ 0 & 0 & 0 & 1 & 0 & 0 \\ 0 & 0 & 0 & 0 & 1 & 0 \\ 0 & 0 & 0 & 0 & 0 & 1 \end{bmatrix} \tag{60}$$

Thus the parameter β_r for the basic edge-event algorithm is selected as $\beta_r = 0.6$ for each edge trigger function. In the Zeno-free edge-event algorithm, the parameter η_1 and η_2 are chosen as $\eta_1 = 0.71$ and $\eta_2 = 0.28$, then we also set $\beta_r = 0.6$ for the trigger function (47) in the Zeno-free trigger algorithm. The minimal inter-edge-event time b_r is chosen as $b_r = 0.0336s$, which satisfies the condition (48).

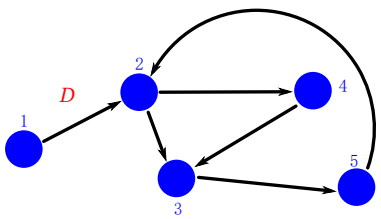

Figure 6: Directed graph topology.

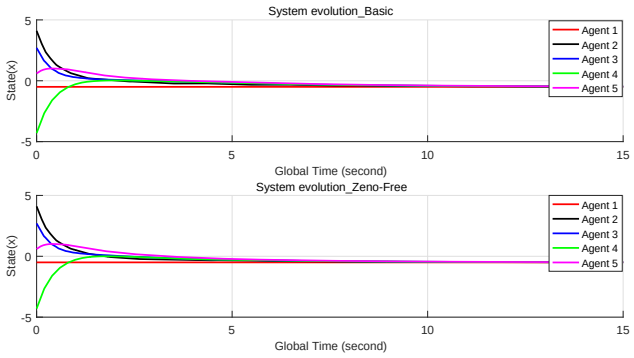

Figure 7: Comparison of state trajectories.

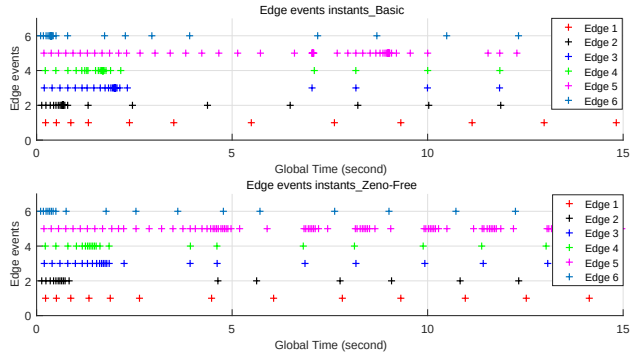

Figure 8: Comparison of edge event times.

Table 2: Comparison of numbers of edge events.

Number of edge	Basic	Zeno-free
Edge 1	12	13
Edge 2	52	18
Edge 3	56	24
Edge 4	53	22
Edge 5	104	91
Edge 6	53	19
Total	330	187

The state trajectories and trigger performance for both the basic algorithm and the Zeno-free algorithm are compared in Fig. 7 and 8, respectively. Table 2 compares the edge event numbers for each edge between the basic algorithm and the Zeno-free algorithm. Note that the minimum inter-edge-event time interval we observed in the simulation of the

basic algorithm is $1 \times 10^{-6} s$, which is the numerical accuracy we set in Matlab. This dense triggering behaviour is observed when the state term $z_r(t)$ crosses zero, which supports the analysis of Zeno behaviour in [14] (see its Remark 2). The minimum inter-edge-event time interval observed in the simulation of the Zeno-free algorithm is $0.0383s$, which corresponds to the value of b_r calculated in the last paragraph.

5 Unsynchronized clock case

5.1 Problem formulation

In this section, we still assume that continuous local relative information is available to each agent. Graph $\mathcal{G}$ is also undirected and connected. Let $t,\ t(0) = 0$ denote the global clock. However, each agent i has its own isolated, local clock $t^i,\ i = 1, 2, \ldots, n$. Let $t^i(0) \geq 0$ denote the initial value for each t^i and $t^i(0), \forall i$ is not necessarily identical. That is to say, agents i and j linked by edge ϵ_r start to measure the relative information and update their control inputs under their own clocks with non-identical initial time. The main challenge in this section arises from the fact that agent i and j linked by ϵ_r do not update their control inputs synchronously.

The MAS we study in this section also consists of n single integrators labelled from 1 to n. Let $x_i(t^i) \in \mathbb{R}$ denote the state of agent $i,\ i = 1, 2, \ldots n$. The dynamics of agent i are given as

$$\dot{x}_i(t^i) = u_i(t^i),\ \ i = 1, 2, \ldots, n, \tag{61}$$

where $u_i(t^i)$ is control input.

Note that the trigger times of the agents i and j linked by ϵ_r are non-identical, we define two time sequences of event-triggered executions for agents i and j, respectively, which are $t^i_{0^i_r}, t^i_{1^i_r}, \ldots, t^i_{k^i_r}, \ldots$ for agent i under t^i and $t^j_{0^j_r}, t^j_{1^j_r}, \ldots, t^j_{k^j_r}, \ldots$ for agent j under t^j. $t^i_{k^i_r}$ denotes the time of k-th edge event of agent i triggered over edge ϵ_r under agent i's clock. Both agents update their control inputs at their own edge event times. For agent i, which is one agent of the agent pair (i, j) linked by ϵ_r, the control input is designed as follows:

$$u_i(t^i) = \sum_{j \in N_i} \left(x_j(t^i_{k^i_r}) - x_i(t^i_{k^i_r}) \right),\ \ i = 1, 2, \ldots, n \tag{62}$$

for $t^i \in [t^i_{k^i_r}, t^i_{k^i_r+1})$. In this section, we will aim to design a new Zeno-free trigger scheme to determine the trigger times.

5.2 Main result

For time $t^i \in [t^i_{k^i_r}, t^i_{k^i_r+1})$, agent i, which is one agent of edge ϵ_r, measures the relative states $z^i_r(t^i)$ continuously along its own time axis and the relative state measurement error is defined as

$$e^i_r(t^i) = z^i_r(t^i_{k^i_r}) - z^i_r(t^i). \tag{63}$$

Since $t^i_{0^i_r} = t^j_{0^j_r}$ can not be guaranteed for agent i and j linked by ϵ_r, it is obvious that $e^i_r(t^i)$ is not supposed to be equal to $e^j_r(t^j)$. When combined the trigger conditions proposed below, it is implied that the linked agents i and j update their controllers asynchronously.

We follow the same method used in the Zeno-free algorithm of Section 3 to determine the next edge event time over ϵ_r for agent i:

$$t^i_{k^i_r+1} = t^i_{k^i_r} + \max\{\tau^i_{k^i_r}, b_r\}. \tag{64}$$

The trigger function used to determine $\tau^i_{k^i_r}$ is proposed as follows:

$$f(e^i_r(t^i), z^i_r(t^i)) = \|e^i_r(t^i)\| - \beta^i_r \|z^i_r(t^i)\| \tag{65}$$

where $\beta^i_r > 0$. As usual, every time the trigger condition (64) is satisfied, $e^i_r(t^i)$ is reset to zero.

Theorem 5. *Consider system* (61) *with control input* (62)*, trigger function* (64)*. Let* η_1 *and* η_2 *be positive real numbers and* $\eta_1 + \eta_2 < 1$*. Let* $\alpha = \max\{\|HH^T_{\otimes}\|, \|HH^T_{\odot}\|\}$*. If* $\beta^i_r \leq \eta_1\lambda_2(L)/2\alpha$ *for all edges,* b_r *is strictly positive and satisfies*

$$b_r \leq \frac{\eta_2\lambda_2(L)}{2\alpha(2m\alpha + \eta_2\lambda_2(L))}. \tag{66}$$

Then

- *(Consensus) All agents' states will reach consensus.*
- *(Zeno-free triggers) No agent will exhibit Zeno behaviour.*

Proof. It is obvious that we do not need to consider the convergence of the system before all agents are activated. Thus we introduce a new global clock t', where $t'(0) = \max\{t^i(0) : i = 1, 2, \ldots, n\}$ indicating the time point that all agents are activated to achieve consensus. Note that the compact form (38) cannot be used here because agents i and j linked by edge ϵ_r update asynchronously. New variables are required to be defined to construct the compact form of the system.

Note that all the state variables used and defined in the proof are with respect to a global coordinate frame. We start the analysis from the continuous-time consensus dynamic $\dot{x}(t') = -H^T z(t')$, as well. In this dynamic, the entry h_{ar}^T of H^T can be explained as follows:

$$h_{ar}^T = \begin{cases} 1, & \text{agent } a\text{'s knowledge of } z_r(t') \text{ is } -z_r(t') \\ -1, & \text{agent } a\text{'s knowledge of } z_r(t') \text{ is } z_r(t') \\ 0, & \text{agent } a \text{ does not access } z_r(t'). \end{cases} \tag{67}$$

Note that $h_{ar}^T = h_{ra}$, h_{ra} is the entry of H. According to the definition of h_{ra} in (67), we have the following conclusions: if agent a is the terminal agent of edge ϵ_r, its knowledge of $z_r(t')$ is $-z_r(t')$; if agent a is the initial agent of edge ϵ_r, its knowledge of z_r is $z_r(t')$. Let the relative states assigned to initial agent i and terminal agent j linked by edge ϵ_r be respectively described by z_r^μ and z_r^ν, where the initial agent and terminal agent are pre-assigned by incidence matrix H. It is obvious that $z_r^\mu(t') = z_r^\nu(t') = z_r(t')$. Note that there are m initial agents and m terminal agents in the MAS since the graph $\mathcal{G}$ has m edges. Then it is reasonable to rewrite the consensus dynamic as $\dot{x} = -H_{\otimes}^T z^\mu(t') - H_{\odot}^T z^\nu(t')$, where $z^\mu = [z_1^\mu, z_2^\mu, \ldots, z_m^\mu]^T$ and $z^\nu = [z_1^\nu, z_2^\nu, \ldots, z_m^\nu]^T$.

Let $t'_{k_r^\mu}$ and $t'_{k_r^\nu}$ re-denote the latest r-th edge event time instants of initial agent i and terminal agent j linked by edge ϵ_r, respectively. It is assumed that $t'_{k_r^\mu}, t'_{k_r^\nu} \geq t'(0)$. Following the consensus dynamic constructed in the last paragraph, the compact form of the control input (62) can be expressed as:

$$u(t') = -H_{\otimes}^T \begin{bmatrix} z_1^\mu(t'_{k_1^\mu}) \\ z_2^\mu(t'_{k_2^\mu}) \\ \vdots \\ z_m^\mu(t'_{k_m^\mu}) \end{bmatrix} - H_{\odot}^T \begin{bmatrix} z_1^\nu(t'_{k_1^\nu}) \\ z_2^\nu(t'_{k_2^\nu}) \\ \vdots \\ z_m^\nu(t'_{k_m^\nu}) \end{bmatrix}, \tag{68}$$

which is the key step of the analysis in the whole proof.

According to (63), we define two stack measurement error vectors $e^\mu = [e_1^\mu, e_2^\mu, \ldots, e_m^\mu]^T$ and $e^\nu = [e_1^\nu, e_2^\nu, \ldots, e_m^\nu]^T$ are defined for all of the initial agents and terminal agents, respectively. The compact form of the consensus dynamic at t' can be formulated as

$$\begin{aligned} \dot{x}(t') &= -H_{\otimes}^T z(t') - H_{\odot}^T z(t') - H_{\otimes}^T e^\mu(t') - H_{\odot}^T e^\nu(t') \\ &= -H^T z(t') - H_{\otimes}^T e^\mu(t') - H_{\odot}^T e^\nu(t') \end{aligned} \tag{69}$$

Now reconsider the Lyapunov function

$$V(t') = \frac{1}{2} z(t')^T z(t')$$

Its time derivative along (69) is

$$\begin{aligned}\dot{V}(t') &= z(t')^T H\dot{x}(t') \\ &= -z(t')^T HH^T z(t') - z(t')^T HH_{\bigotimes}^T e^{\mu}(t') \\ &\quad - z(t')^T HH_{\bigodot}^T e^{\nu}(t')\end{aligned}$$

By recalling Lemma 2.2, it yields that

$$\begin{aligned}\dot{V}(t') &\leq -\lambda_2(L)\|z(t')\|^2 + \|HH_{\bigotimes}^T\|\|z(t')\|\|e^{\mu}(t')\| \\ &\quad + \|HH_{\bigodot}^T\|\|z(t')\|\|e^{\nu}(t')\| \\ &= -\left(\lambda_2(L)\|z(t')\| - \|HH_{\bigotimes}^T\|\|e^{\mu}(t')\|\right. \\ &\quad \left.-\|HH_{\bigodot}^T\|\|e^{\nu}(t')\|\right)\|z(t')\|\end{aligned}$$

Note that $\|e^{\mu}(t')\| = \sqrt{\sum_{r=1}^{m}\|e_r^{\mu}(t')\|^2}$ and $\|e^{\nu}(t')\| = \sqrt{\sum_{r=1}^{m}\|e_r^{\nu}(t')\|^2}$. Let $\alpha = \max\{\|HH_{\bigotimes}^T\|, \|HH_{\bigodot}^T\|\}$. If we can ensure the following condition

$$\sqrt{\sum_{r=1}^{m}\|e_r^{\mu}(t')\|^2} + \sqrt{\sum_{r=1}^{m}\|e_r^{\nu}(t')\|^2} \leq \frac{\lambda_2(L)}{\alpha}\|z(t')\| \tag{70}$$

then consensus will be achieved.

At t', let $S_{\mu}^1(t')$ and $S_{\mu}^2(t')$ be the edge sets that their linked initial agents will trigger the edge events at $t'_{k_r^{\mu}} + \tau_{k_r^{\mu}}$ and $t'_{k_r^{\mu}} + b_r$, respectively. It is satisfied that $S_{\mu}^1(t') \bigcup S_{\mu}^2(t') = \{\epsilon_1, \ldots, \epsilon_m\}$ and $S_{\mu}^1(t') \bigcap S_{\mu}^2(t') = \emptyset$. Similarly, let $S_{\nu}^1(t')$ and $S_{\nu}^2(t')$ denote the edge sets that their linked terminal agents will trigger the edge events at $t'_{k_r^{\mu}} + \tau_{k_r^{\mu}}$ and $t'_{k_r^{\mu}} + b_r$, respectively. it is also satisfied that $S_{\nu}^1(t') \bigcup S_{\nu}^2(t') = \{\epsilon_1, \ldots, \epsilon_m\}$ and $S_{\mu}^1(t') \bigcap S_{\mu}^2(t') = \emptyset$. Note that condition (70) can be guaranteed if

$$\sqrt{\sum_{r\in S_{\mu}^1(t')}\|e_r^{\mu}(t')\|^2} + \sqrt{\sum_{r\in S_{\nu}^1(t')}\|e_r^{\nu}(t')\|^2} \leq \frac{\eta_1\lambda_2(L)}{\alpha}\|z(t')\| \tag{71}$$

and

$$\sqrt{\sum_{r\in S_{\mu}^2(t')}\|e_r^{\mu}(t')\|^2} + \sqrt{\sum_{r\in S_{\nu}^2(t')}\|e_r^{\nu}(t')\|^2} \leq \frac{\eta_2\lambda_2(L)}{\alpha}\|z(t')\| \tag{72}$$

where $\eta_1, \eta_2 > 0$ and $\eta_1 + \eta_2 < 1$.

According to the trigger function (65) and the fact that the measurement error (63) is reset as soon as the value of the trigger function reaches zero, it is enough to imply $\|e_r^{\mu}(t')\| \leq \beta_{\max}\|z_r(t')\|$ and $\|e_r^{\nu}(t')\| \leq \beta_{\max}\|z_r(t')\|$, where $\beta_{\max} = \max\{\beta_r^i\}$. Furthermore,

by recalling that $S_\mu^1(t')$ and $S_\nu^1(t')$ are subsets of edge set $\mathcal{E}$, we obtain $\mathbf{card}\{S_\mu^1(t')\}$, $\mathbf{card}\{S_\nu^1(t')\} \leq m$. The above analysis indicates that the upper bound of the left-hand side term in (71) can be calculated as $2\sqrt{\sum_{r=1}^m \beta_{\max}^2 \|z_r(t')\|^2}$, which is equal to $2\beta_{\max}\|z(t')\|$. If we enforce β_r^i to satisfy $\beta_r^i < \frac{\eta_1\lambda_2(L)}{2\alpha}$, then condition (71) is always satisfied.

For condition (72), since $\mathbf{card}\{S_\mu^2(t')\} \leq m$, we obtain $\sqrt{\sum_{r\in S_\mu^2(t')} \|e_r^\mu(t')\|^2} \leq \sum_{r=1}^m \|e_r^\mu(t')\|$. According to the same arguments, we also get $\sqrt{\sum_{r\in S_\nu^2(t')} \|e_r^\mu(t')\|^2} \leq \sum_{r=1}^m \|e_r^\nu(t')\|$. The upper bound of the left-hand side term in (72) is thus obtained as $\sum_{r=1}^m \|e_r^\mu(t')\| + \sum_{r=1}^m \|e_r^\nu(t')\|$. Note that $e_r^\mu(t')$ and $e_r^\nu(t')$ are actually the measurement error $e_r^i(t')$ defined in (63). By enforcing $\|e_r^i(t')\| \leq \frac{\eta_2\lambda_2(L)}{2m\alpha}\|z(t')\|$, condition (72) can be ensured. Now we are ready to determine B_r. By following the similar process from (56) to (58) in the last subsection, the lower bound B_r is obtained as

$$B_r = \frac{\eta_2\lambda_2(L)}{2\alpha(2m\alpha + \eta_2\lambda_2(L))} \tag{73}$$

For each agent i, the next edge-triggering time $t_{k_r^i+1}^i$ can be set as $t_{k_r^i}^i + b_r$, where $b_r \leq B_r$, if $\tau_{k_r^i}^i$ determined by trigger function (65) is less than b_r. By choosing suitable β_r and b_r, the aims of both consensus and Zeno-free triggers can be achieved. □

5.3 Simulation

The sensing topology and the initial states of all agents are set to be same to with those in the simulation of Section 3. Parameters η_1 and η_2 are chosen as $\eta_1 = 0.8$ and $\eta_2 = 0.19$. Thus β_r^i and minimum inter-event time b_r are calculated as $\beta_r^i = 0.22$ and $b_r = 0.0011s$, respectively. The activated times for all agents are chosen as $t^1(0) = 0.4$, $t^2(0) = 0.7$, $t^3(0) = 0.1$, $t^4(0) = 0.2$ and $t^5(0) = 0.8$. Fig. 9 illustrates the trajectories of the MAS. We can see consensus can be reached. Fig. 10 shows the trigger time instants for both agent 1 and agent 2 over edge ϵ_1. It can be observed that their trigger times are asynchronous.

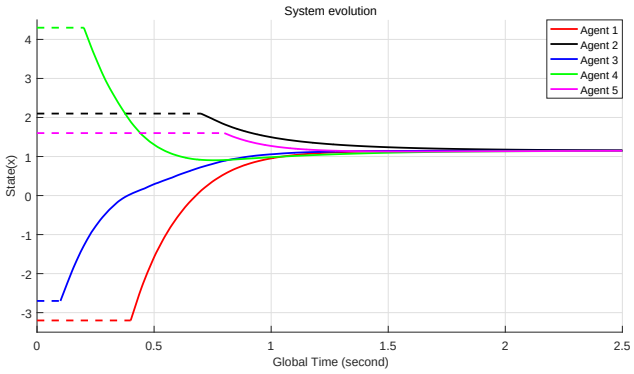

Figure 9: State trajectories.

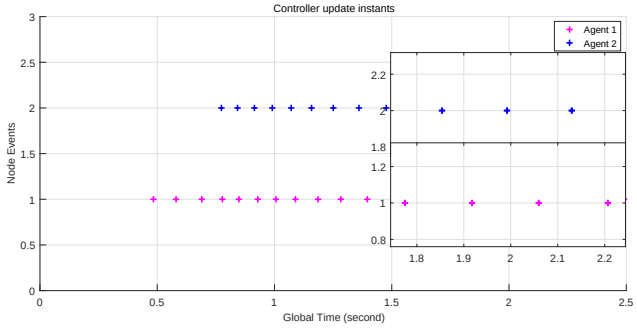

Figure 10: Edge event times of both agent 1 and agent 2 triggered over edge ϵ_1.

6 Conclusion and future work

6.1 Conclusion

In this report, we propose novel Zeno-free, edge-event-based algorithms to achieve multi-agent consensus under both synchronized clocks and unsynchronized clocks. In the synchronized clock case, we show that average consensus can be achieved under our proposed algorithms even though each agent can only measure the relative information in its own local coordinate frame via undirected sensing topologies. In addition, the MAS is also proved to reach consensus in directed sensing topologies. In the study of the unsynchronized clock case, each agent not only uses the relative information, but also works under its own clock that is not necessarily synchronized with others' clocks. We show that consensus can be achieved with Zeno-free triggers by using our proposed algorithm.

6.2 Future work

The near future research topics will be discussed in the part.

- **Edge-event-based control for complex dynamics**
  Since the dynamics of real autonomous systems are quiet complex, the multi-agent system modeled by complex dynamics should be investigated. We first consider agents by second-order dynamics, and then extend the result to general nonlinear dynamics. It is obvious that complex systems pose more theoretical challenges than the networked systems modeled by simple dynamics.

- **Edge-event-based control for unsynchronized multi-agent system with sampled-data setting**
  In event-based control (edge-event and node-event schemes), event detector has to continuously measure the relative states of neighboring agents among the network or self-state as mentioned above. However, sampled-data control strategy can be applied to avoid continuous measurement completely and Zeno-behavior can also be eliminated automatically. This control scheme is more practical in real applications but also more challenging technically.

- **Cooperative control of multi-agent systems with uncertain interactive information**
  This topic has attracted growing attention among the control community recently, due to its broad applications and increasing demands in many areas. For example, autonomous quadrotors work cooperatively in detecting the high voltage line and the sensors may be interfered by electromagnetic. For this topic, uncertain interactive information (interactive information with noise or random switch sensing topologies) of each agent is deserved to be studied in cooperative control. There are still few systematic and theoretical frameworks for cooperative control of MASs with uncertain interactive information.

References

[1] W. Ren and R. W. Beard, *Distributed consensus in multi-vehicle cooperative control*. Springer, 2008.

[2] J. Qin, Q. Ma, Y. Shi, and L. Wang, "Recent advances in consensus of multi-agent systems: A brief survey," *Industrial Electronics, IEEE Transactions on*, vol. pp, pp. 1–1, December 2016.

[3] N. Huang, Z. Duan, and G. Chen, "Some necessary and sufficient conditions for consensus of second-order multi-agent systems with sampled position data," *Automatica*, vol. 63, no. 1, pp. 214 – 155, 2016.

[4] J. Qin and H. Gao, "A sufficient condition for convergence of sampled-data consensus for double-integrator dynamics with nonuniform and time-varying communication delays," *IEEE Transactions on Automatic Control*, vol. 57, no. 9, pp. 2417–2422, 2012.

[5] D. V. Dimarogonas, E. Frazzoli, and K. H. Johansson, "Distributed event-triggered control for multi-agent systems," *Automatic Control, IEEE Transactions on*, vol. 57, no. 5, pp. 1291 – 1297, 2012.

[6] Y. Fan, G. Feng, Y. Wang, and C. Song, "Distributed event-triggered control of multi-agent systems with combinational measurements," *Automatica*, vol. 49, no. 2, pp. 671 – 675, 2013.

[7] F. Xiao, X. Meng, and T. Chen, "Average sampled-data consensus driven by edge events," in *Chinese Control Conference, 2012. 31st IEEE Conference on*, pp. 6239 – 6244, IEEE, 2012.

[8] G. S. Seyboth, D. V. Dimarogonas, and K. H. Johansson, "Event-based broadcasting for multi-agent average consensus," *Automatica*, vol. 49, no. 1, pp. 245–252, 2013.

[9] C. Nowzari and J. Cortés, "Zeno-free, distributed event-triggered communication and control for multi-agent average consensus," in *American Control Conference (ACC), 2014*, pp. 2148–2153, IEEE, 2014.

[10] F. Xiao, X. Meng, and T. Chen, "Sampled-data consensus in switching networks of integrators based on edge events," *International Journal of Control*, vol. 88, no. 2, pp. 391 – 402, 2015.

[11] Y. Fan, L. Liu, G. Feng, and L. Wang, "Self-triggered consensus for multi-agent systemswith zeno-free triggers," *Automatic Control, IEEE Transactions on*, vol. 60, no. 10, pp. 2779 – 2784, 2015.

[12] Q. Liu, J. Qin, and C. Yu, "Event-based multi-agent cooperative control with quantized relative state measurements," in *Decision and Control, 2016. 55th IEEE Conference on*, pp. 2233 – 2239, IEEE, 2016.

[13] B. Wei, F. Xiao, and M.-Z. Dai, "Edge event-triggered control for multi-agent systems under directed communication topologies," *International Journal of Control*, vol. 0, no. 0, pp. 1–10, 0.

[14] Z. Sun, N. Huang, B. D. O. Anderson, and Z. Duan, "A new distributed zeno-free event-triggered algorithm for multi-agent consensus," in *Decision and Control, 2016. 55th IEEE Conference on*, pp. 3444 – 3449, IEEE, 2016.

[15] R. Carli and S. Zampieri, "Networked clock synchronization based on second order linear consensus algorithms," in *Decision and Control (CDC), 2010 49th IEEE Conference on*, pp. 7259–7264, IEEE, 2010.

[16] G. S. Seyboth and F. Allgower, "Clock synchronization over directed graphs," in *Decision and Control (CDC), 2013 IEEE 52nd Annual Conference on*, pp. 6105–6111, IEEE, 2013.

[17] G. Seyboth, "Event-based control for multi-agent systems," *Master's Degree Project, Stockholm, Sweden*, 2010.

[18] Z. Zeng, X. Wang, and Z. Zheng, "Edge agreement of multi-agent system with quantised measurements via the directed edge laplacian," *Control Theory & Application, IET*, vol. 10, pp. 1583 – 1589, August 2016.

[19] M. Guo, "Quantized cooperative control," *Master's Degree Project, Stockholm, Sweden*, 2011.

[20] K. Thulaslraman and M. Swamy, *Graphs: Theory and algerithms*. Wiley, 2011.

[21] P. Tabuada, "Event-triggered real-time scheduling of stabilizing control tasks," *Automatic Control, IEEE Transactions on*, vol. 52, pp. 1680–1685, September 2007.